EPJ Web of Conferences **182**, 02122 (2018) https://doi.org/10.1051/epjconf/201818202122
ICNFP 2017

Observation of ultra-high energy cosmic rays with the Telescope Array experiment

Ryuji Takeishi[1,a] on behalf of the Telescope Array collaboration

[1] *Institute for Cosmic Ray Research, University of Tokyo, Kashiwa, Chiba, Japan*

Abstract. The origin of ultra-high energy cosmic rays (UHECRs) has been a long-standing mystery. The Telescope Array (TA) is the largest experiment in the northern hemisphere observing UHECR in Utah, USA. It aims to reveal the origin of UHECR by studying the energy spectrum, mass composition and anisotropy of cosmic rays. TA is a hybrid detector comprised of three air fluorescence stations which measure the fluorescence light induced from cosmic ray extensive air showers, and 507 surface scintillator counters which sample charged particles from air showers on the ground. We present the cosmic ray spectrum observed with the TA experiment. We also discuss our results from measurement of the mass composition. In addition, we present the results from the analysis of anisotropy, including the excess of observed events in a region of the northern sky at the highest energy. Finally, we introduce the TAx4 experiment which quadruples TA, and the TA low energy extension (TALE) experiment.

1 Introduction

Ultra-high energy cosmic rays (UHECRs) are cosmic rays with energies larger than about 10^{18} eV. The flux of cosmic rays follows power law distribution, and due to low flux, the origin of UHECR is unrevealed. UHECRs are observed by using cascade reactions of primary cosmic rays with atmospheric particles, which are called air showers. Using air shower particle information observed on the ground and an air shower Monte-Carlo (MC) simulation, the energy and arrival direction of primary cosmic rays are reconstructed. One of the methods to observe air showers is to use a surface detector (SD) array, which samples charged particles on the ground. Another method is performed by a fluorescence detector (FD), which measures fluorescence light generated by air shower development in the sky.

One of the uncertainties in UHECR observation derives from the hadronic interaction model used for air shower MC simulations. Since UHECR energy range is beyond accelerator experiments, hadronic interaction models used in air shower MCs adopt extrapolated values for interaction parameters, such as cross section and multiplicity, from lower energy experimental data. The Pierre Auger Observatory reported that the simulated number of muons from UHECR air showers on the ground shows a deficit of 30 to $80\%^{+17}_{-20}(\mathrm{sys})\%$, depending on the model, compared to the observed number [2]. Another study from the Auger experiment also describes the discrepancy between observed hadronic signals and simulated [3]. They suggest present hadronic models used in air shower MCs do not fully reproduce UHE air showers.

[a] e-mail: take@icrr.u-tokyo.ac.jp

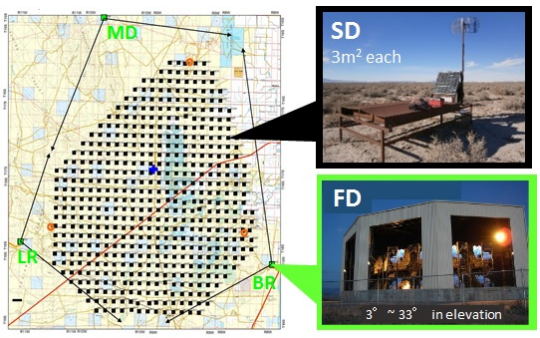

Figure 1. Layout of the Telescope Array experiment. An SD array of 507 scintillation counters are surrounded by 3 FD stations, named MD, BR and LR.

The Telescope Array (TA) is the largest cosmic ray observatory in the Northern hemisphere [1]. It is located in Millard County, Utah, USA at about 39.30° north latitude, 112.91° west longitude and 1400m altitude. The experiment consists of an array of 507 scintillator SDs, which has an area greater than 700km^2, and 38 FD telescopes in 3 stations overlooking the SD array. The main part of the Telescope Array was operational as of 2008. The layout of the TA experiment is shown in figure 1.

The TA SD is 3 m^2 each in area, located in a square grid of 1.2 km spacing [4]. Each SD has two layers of scintillators under the iron roof. Wavelength shifting fibers are placed on the scintillators and they guide the scintillation light to two PMTs, one for each layer. The SDs are solar-powered and the cosmic ray signals are sent by a 2.4 GHz radio system. The duty cycle of the SDs is approximately 100%.

The northern FD station has 14 telescopes, re-utilizing telescopes from the High Resolution Fly's Eye (HiRes) experiment [5]. Each telescope has 5.1 m^2 spherical mirror which images the air shower onto a camera. The Field of View (FoV) is $3° - 31°$ in elevation and 112° in azimuth direction. Each of the southern two stations has 12 telescopes, each with 6.8 m^2 mirror [6]. They have $3° - 33°$ FoV in elevation and 108° in azimuth direction for each station. A camera of FDs in three stations consists of 256 hexagonal PMTs in a 16×16 honeycome array. The fluorescence light from air showers is collected by the mirrors and viewed by PMTs through a UV band-pass filter. The signal is digitized and read out by electronics, which trigger cosmic ray signal patterns. Due to the high sensitivity of the telescopes and cameras to the light, the FD is only operated on clear moonless nights. The duty cycle of the FDs is about 10%.

The scientific goal of TA is to reveal the origin of UHECR by determining the energy spectrum of UHECR, their mass composition, and investigation of anisotropies of UHECR in the Northern sky. In this paper we will present the results based on the analysis of the 9 years of TA data.

2 Energy spectrum

For the measurement of the spectrum of UHECR, the high quality SD events within the zenith angle 45° have been selected [7]. The air shower energy and geometry are reconstructed from particle signal size and arrival time distributions measured with the SDs. Fits to the time and signal distribution as a function of the distance perpendicular to an air shower track determine the air shower direction and the density of shower particles at the distance of 800 m, which is called S800, respectively. The

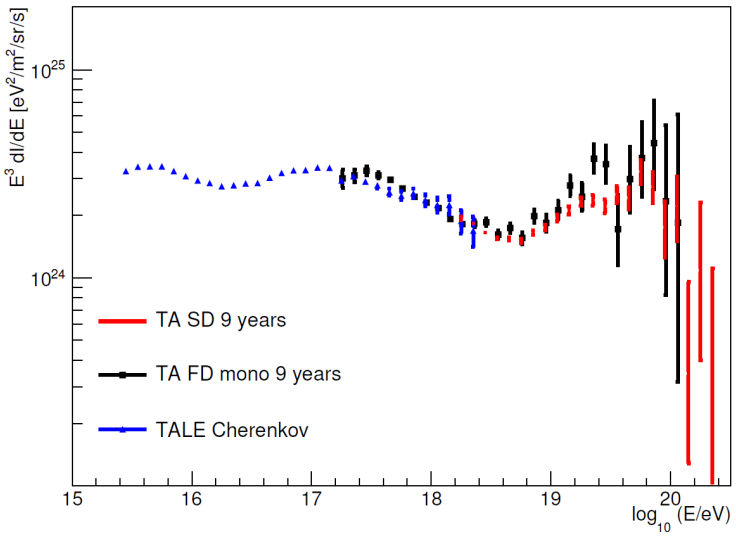

Figure 2. TA energy spectrum for 9 years data [8].

energy is then estimated by using a look-up table in S800 and the zenith angle of the shower from a MC simulation.

We see the difference between the reconstructed energy with the SD data and the energy observed by the TA FD by 27%, using events seen in common between the SD and FD. The energy scale uncertainty of the FD is experimentally well-controlled, since it uses a calorimetric determination. We therefore correct our energy scale to the FD. The angular resolution and energy resolution of the TA SD reconstruction for $E > 10^{19}$ eV are 1.4° and < 20%, respectively.

Figure 2 shows the spectrum measured by the TA SD [8]. It agrees very well with the previous measurements by the HiRes experiment. One can see the suppression structure at the highest energy. A fit to a broken power law shows a change in the spectrum index from 2.69 ± 0.02 to 4.63 ± 0.49 at $10^{19.81\pm0.04}$ eV. The significance of the cutoff is inferred by a linear extrapolation of the power law beyond the suppression energy. The expected number of events beyond the cutoff energy is 79.8, while observed value is 26. This difference corresponds to a Poisson probability 2.2×10^{-12}, or 6.9σ. It indicates the GZK cutoff, which is the flux reduction by the reaction between cosmic rays and cosmic microwave background photons [9, 10]. The ankle structure is also found in $10^{18.69\pm0.02}$ eV, where the spectrum index below the energy is 3.27 ± 0.03. This can be explained by e^+e^- pair production above the ankle.

The spectrum measured by the TA FD is also shown in the figure, which is consistent with the SD data in the overlap region. The spectrum measured by the Auger experiment is also in good agreement with the TA spectra if the energy scaling is performed by about 10%. However, the cutoff point of the Auger spectrum is significantly lower than the TA spectrum. This discrepancy is the remaining problem of the spectrum measurement.

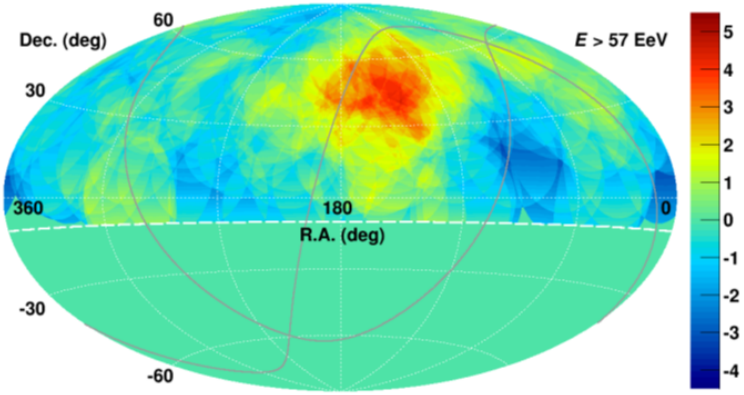

Figure 3. Aitoff projection of the UHECR map in equatorial coordinates with energy $E > 57$ EeV. The solid curves indicate the galactic plane (GP) and supergalactic plane (SGP). The color contour shows the significance of the excess of the number of events to the isotropic background events generated by a MC.

3 Anisotropy

For the anisotropy study, loosened selection criteria for the SD events have been compiled in order to increase statistics [11]. Figure 3 shows a sky map in equatorial coordinates with energy $E > 57$ EeV observed by the TA SD data. Using the 9 years data, we observe 143 events with the energy region. These events are oversampled with 25°, then we find a region where 34 events are inside. The center of the region is 144.3° in right ascension and 40.3° in declination. We generate a MC simulation, which includes detailed detector responses, and expect 13.5 events as a background in this area assuming an isotropic arrival direction. The Li-Ma significance is 5.06σ. Using large statistics of MC datasets which assume a uniform distribution over the TA exposure, we calculate a chance probability that this excess could appear by a statistical fluctuation. The chance probability is 2.96σ, and we call this excess as a hotspot. The hotspot could indicate the source of UHECRs, while we cannot rule out the relation between the excess and nearby astrophysical objects.

4 Mass composition

We estimate the mass composition of cosmic rays using $X_{\rm max}$, the atmospheric depth of the maximum of the air shower. Lighter composition has a larger energy per nucleon than heavier nuclei at the same energy. Hence proton showers develop deeper and have larger $X_{\rm max}$ than heavier nuclei. The air shower longitudinal development can be measured by the FD, so the TA FD data are used for the composition analysis. Because of the large fluctuations of air showers, the composition can only be inferred from statistical quantities of $X_{\rm max}$.

TA utilizes deferent analysis techniques using three independent FD stations and the SD array. The hybrid analysis uses the FD and SD data to constrain the geometry of air showers. In the analysis, one combines the arrival time and core location information measured by the SD, and the shower geometry can be well measured comparing the analysis using monocular FD data. The stereo analysis is one of the other methods to measure the composition, which utilizes the data of two FD stations. Each detector measures a shower-detector plane, and by determining the line crossing the planes, the air shower track is constrained accurately.

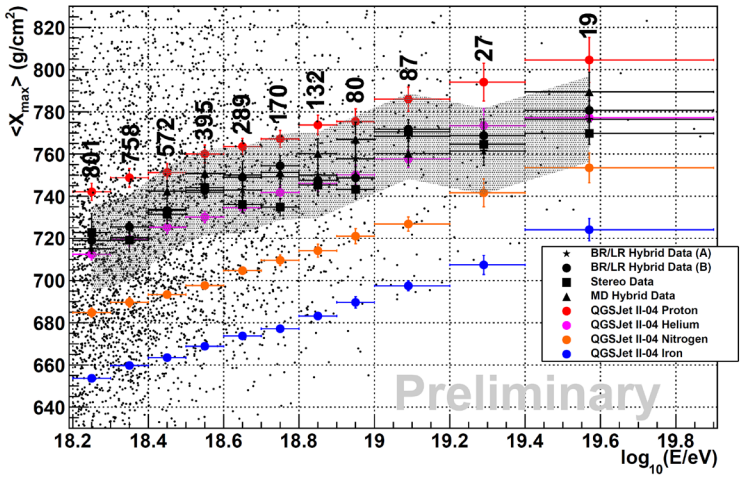

Figure 4. $X_{\max}$ distribution as a function of primary cosmic ray energy [13]. Black points show the TA data. Different markers mean different analysis methods. BR and LR hybrid analyses have been performed independently by two methods, in order to understand systematic uncertainties about air shower reconstruction. The gray band indicates systematic uncertainties of 20.3 g/cm^2 on BR/LR hybrid data. Event numbers of the BR/LR hybrid data (A) are also shown.

We generate a MC air shower simulation by CORSIKA [12] to expect the distribution of $X_{\max}$. The generated showers are then run through the reconstruction procedure identical to that used for the experimental data including the full simulation of the detector. For the BR/LR hybrid analysis, the $X_{\max}$ resolution for protons is no greater than 20 g/cm^2 and no greater than 15 g/cm^2 for iron [13]. For the MD hybrid analysis, the $X_{\max}$ resolution is $\sim$ 22 g/cm^2 [13].

Figure 4 shows the measured $X_{\max}$ and expected values for MCs in several models. Eight and seven year data are used for BR/LR hybrid and MD hybrid analysis, respectively. The experimental data using different methods are compatible with each other within systematics. The result indicates a light component for primary cosmic rays.

5 Hadron interaction

The muon excess measured by the Auger experiment [2, 3] suggests that present hadronic models do not fully reproduce air showers. One may test the hadronic interaction models by comparing the measured number of muons with the MC prediction. We study muons in UHE air showers using the TA SD data.

The TA SD is made of plastic scintillator, and it is sensitive to the electromagnetic (EM) components that is the major part of air shower particles. To approach this issue, we used highly inclined shower events which should have a high muon ratio in the SD signal, and compare the observed signal size with the MC prediction. We analyzed events with the energy $10^{18.8}$ eV $< E < 10^{19.2}$ eV using TA SD seven year data. We use the MC for proton primary cosmic rays from the result of TA FD $X_{\max}$ measurements.

The EM components generated on the shower track are composed of electron and gamma, They are attenuated faster than muons compared in the same path length, because their energy is largely

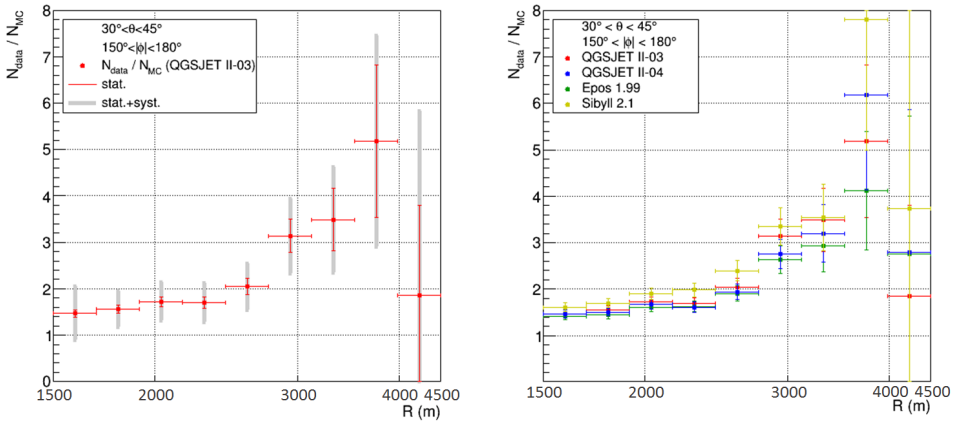

Figure 5. The results of the study of muons from showers using TA SD data [18]. (left) Lateral distribution of the average ratio of the data to the MC on the high muon ratio condition described in the text. The vertical thin error bars and shaded grey thick error bars represent statistical error and quadratic sum of statistical and systematic errors, respectively. (right) Same as the left panel, but for the MC with various hadronic models. The red, blue, green and yellow represent QGSJET II-03, QGSJET II-04, Epos 1.99 and Sibyll 2.1, respectively.

lost during the shower development in the atmosphere. We divide the detector hit in the air shower events of the dataset using θ (the zenith angle), ϕ (the azimuth angle relative to the shower arrival direction projected onto the ground), and R (the distance from shower track). If θ, ϕ and R values become large, the path length between the shower track above the ground and the SD increases, then the SD is expected to have a high ratio of muons to all particle signals. Here we call the ratio as the muon purity.

Using a MC simulation for proton with QGSJET II-03 hadronic model [14], the muon purity is 60 - 70% on the high muon purity condition ($30^\circ < \theta < 45^\circ$, $150^\circ < |\phi| < 180^\circ$, 2000 m $< R <$ 4000 m) [18]. The left panel of figure 5 shows the ratio of the SD signal of the experimental data to the MC prediction as a function of a lateral distance R [18]. The result on the high muon purity condition described above is shown. The signal of the data is larger than the MC by > 1.5 times. The right panel of figure 5 shows the ratio of SD signals to MCs with various hadronic models, QGSJET II-03, QGSJET II-04 [15], Epos 1.99 [16] and Sibyll 2.1 [17]. It also shows that the data are larger than the MCs. The results indicate the number of muons of the data from air showers is larger than the MC, and the MC does not fully reproduce lateral distributions of showers.

6 Future plan

The plan to quadruple the size of the TA experiment is on progress. The TAx4 experiment aims to clarify the details of the hotspot observed at $E > 57$ EeV with new SDs and FDs covering 4 times larger area than the TA. The spectrum and composition at the highest energies are also investigated. New SD part of the expansion has been funded by the Japanese funding agencies since 2015. New FD part has also been funded by the US NSF since 2016.

Figure 6 shows the overview of the TAx4 experimental site. The TA SD has 1.2 km spacing, while the TAx4 SD has 2.08 km spacing to obtain larger detection area. 500 additional scintillator SDs and

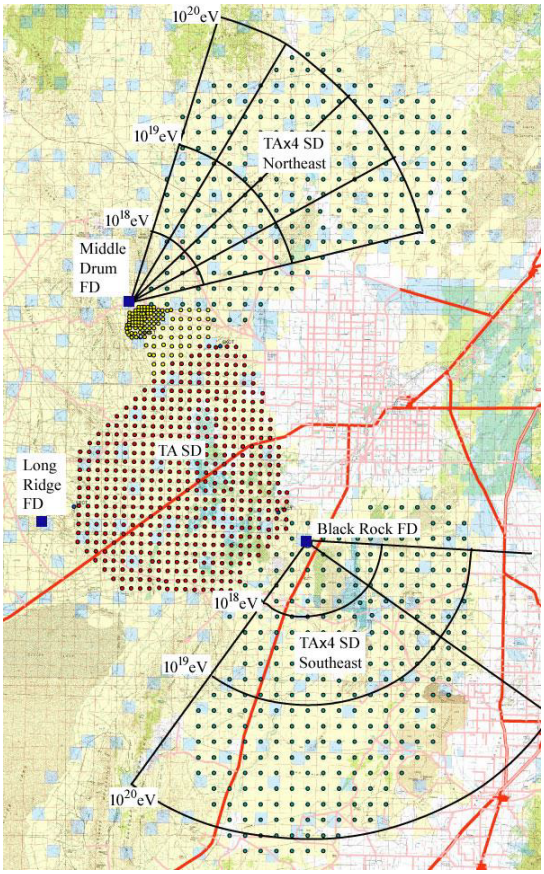

Figure 6. The map of TAx4 experiment. The TA SD array with 1.2 km spacing is shown as red points. The green points are the planned location of the TAx4 SD with 2.08 km spacing. The 2 fan shapes drawn with black lines describe the expected field of view from TAx4 FDs.

TA SDs will cover 3000 km^2. Two additional FDs will observe the sky above the TAx4 SD array located in the North East and South East side of the TA SD array. The energy and angular resolutions at $E > 57$ EeV will be 25% and 2.2°, respectively [19]. We expect the equivalent of 19 years of the TA SD data by 2020.

The Telescope Array Low Energy Extension (TALE) is also on progress. The experiment aims to identify the transition from galactic to extragalactic cosmic ray origin by observing the cosmic ray spectrum and mass composition with the energy around $10^{16} - 10^{18.5}$ eV. Figure 7 shows the map of the TALE site. The experiment consists of 10 FD telescopes observing high elevation (31° – 59°) in the sky located in the MD FD site, and an in-fill array of 103 SDs arranged with spacings that grows with distance from the TALE FD. The spectrum observed by the TALE FD has been analyzed [20].

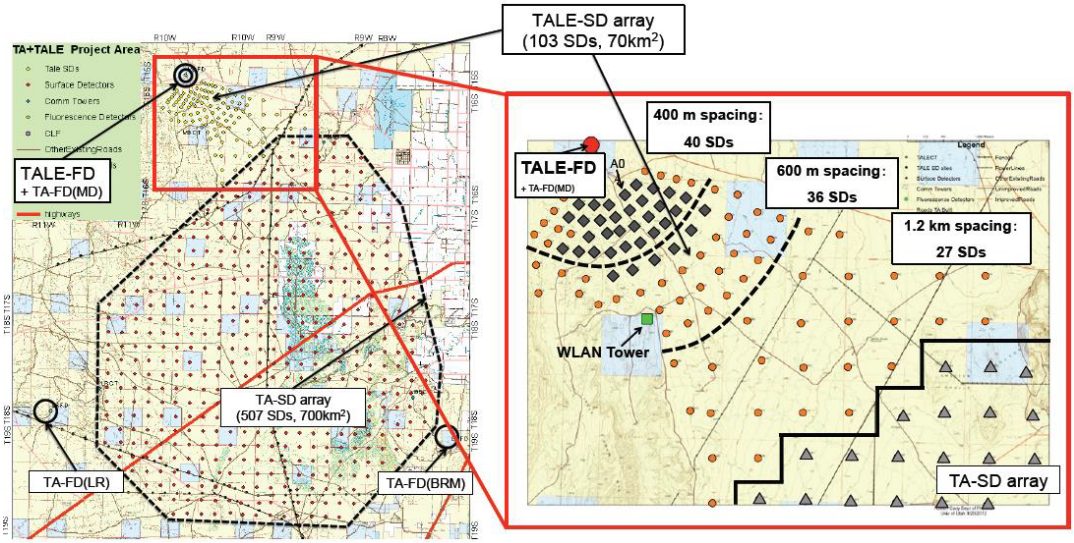

Figure 7. The map of TALE experiment. The TALE SD array is shown as circles and diamonds in the right panel.

7 Summary

The TA experiment has measured the energy spectrum, arrival direction, mass composition and the lateral distribution of high muon purity signals in UHECRs. The spectrum showed cutoff structure at highest energy with 6.9σ significance, which is consistent with the GZK cutoff. We observed a hotsot of the arrival direction in the northern hemisphere at $E > 57$ EeV. The $X_{\max}$ measurement indicates the mass composition is a light component. The study of muons from air showers suggested the muon excess in the experimental data, and the information about more reliable hadronic models for shower MCs has obtained. We need more statistics of cosmic rays at highest energy to reveal the details of the hotspot, and the TAx4 experiment will provide more additional data. The TALE experiment is also in progress to identify galactic to extragalactic transition of cosmic rays.

Acknowledgements

The Telescope Array experiment is supported by the Japan Society for the Promotion of Science through Grants-in-Aid for Scientific Research on Specially Promoted Research (21000002) “Extreme Phenomena in the Universe Explored by Highest Energy Cosmic Rays” and for Scientific Research (19104006), and the Inter-University Research Program of the Institute for Cosmic Ray Research; by the U.S. National Science Foundation awards PHY-0307098, PHY-0601915, PHY-0649681, PHY-0703893, PHY-0758342, PHY-0848320, PHY-1069280, PHY-1069286, PHY-1404495 and PHY-1404502; by the National Research Foundation of Korea (2015R1A2A1A01006870, 2015R1A2A1A15055344, 2016R1A5A1013277, 2007-0093860, 2016R1A2B4014967); by the Russian Academy of Sciences, RFBR grant 16-02-00962a (INR), IISN project No. 4.4502.13, and Belgian Science Policy under IUAP VII/37 (ULB). The foundations of Dr. Ezekiel R. and Edna Wattis Dumke, Willard L. Eccles, and George S. and Dolores Doré Eccles

all helped with generous donations. The State of Utah supported the project through its Economic Development Board, and the University of Utah through the Office of the Vice President for Research. The experimental site became available through the cooperation of the Utah School and Institutional Trust Lands Administration (SITLA), U.S. Bureau of Land Management (BLM), and the U.S. Air Force. We appreciate the assistance of the State of Utah and Fillmore offices of the BLM in crafting the Plan of Development for the site. We also wish to thank the people and the officials of Millard County, Utah for their steadfast and warm support. We gratefully acknowledge the contributions from the technical staffs of our home institutions. An allocation of computer time from the Center for High Performance Computing at the University of Utah is gratefully acknowledged.

References

[1] M. Fukushima *et al.*, Prog. Theor. Phys. Suppl. **151**, 206 (2003)
[2] A. Aab *et al.*, Phys. Rev. D **91**, 032003 (2015)
[3] A. Aab *et al.*, Phys. Rev. Lett. **117**, 192001 (2016)
[4] T. Abu-zayyad *et al.*, Nucl. Instrum. Methods. A **689**, 87-97 (2012)
[5] J. Boyer *et al.*, Nucl. Instrum. Methods. A **482**, 457-474 (2002)
[6] H. Tokuno *et al.*, Nucl. Instrum. Methods. A **676**, 54-65 (2012)
[7] T. Abu-Zayyad *et al.*, ApJ **768**, L1 (2013)
[8] Y. Tsunesada *et al.*, Proc. 35th ICRC, 535 (2017)
[9] K. Greisen, Phys. Rev. Lett. **16**, 748 (1966)
[10] G. T. Zatsepin and V. A. Kuzmin. JETP Lett. **4**, 78 (1966)
[11] R.U. Abbasi *et al.*, ApJL **790**, L21 (2014)
[12] D. Heck *et al.*, Forschungszentrum Karlsruhe Report FZKA, 6019 (1998)
[13] W. Hanlon *et al.*, Proc. 35th ICRC, 536 (2017)
[14] S. Ostapchenko, Nucl. Phys. B, Proc. Suppl. **151**, 147 (2006)
[15] S. Ostapchenko, Phys. Rev. D **83**, 014018 (2011)
[16] T. Pierog and K. Werner, Nucl. Phys. Proc. Suppl. **196**, 102 (2009)
[17] E. J. Ahn *et al.*, Phys. Rev. D **80**, 094003 (2009)
[18] R. Takeishi *et al.*, Proc. 35th ICRC, 313 (2017)
[19] E. Kido *et al.*, Proc. 35th ICRC, 386 (2017)
[20] T. AbuZayyard *et al.*, Proc. 35th ICRC, 534 (2017)